Rapid Communications

Elastoplastic description of sudden failure in athermal amorphous materials during quasistatic loading

Marko Popović,* Tom W. J. de Geus, and Matthieu Wyart†
Institute of Theoretical Physics, École Polytechnique Fédérale de Lausanne (EPFL), CH-1015 Lausanne, Switzerland

(Received 22 April 2018; published 11 October 2018)

The response of amorphous materials to an applied strain can be continuous or instead discontinuous if the initial configuration is very stable. We study theoretically how such a stress drop emerges as the system's initial stability is increased. We show that this emergence is well reproduced by elastoplastic models and is predicted by a mean field approximation, where it corresponds to a continuous transition. In the mean field, failure can be forecasted from the avalanche statistics. We show that this is not the case for very stable materials in finite dimensions due to rare weak regions where a shear band nucleates. To understand the nucleation, we build an analogy with fracture mechanics predicting that the critical nucleation radius of a shear band follows $a_c \sim (\Sigma - \Sigma_b)^{-2}$, where Σ is the stress and Σ_b is the stress that a shear band can carry.

DOI: 10.1103/PhysRevE.98.040901

Introduction. How amorphous solids such as granular materials, bulk metallic glasses, colloidal suspensions, and foams yield under an applied strain is a central question in fields as diverse as geophysics [1], material science [2], and soft matter [3]. At a macroscopic level, the stress versus strain curve under quasistatic loading can (i) monotonically increase, (ii) slightly overshoot as in foams and granular materials [4], or (iii) even be discontinuous as in some metallic glasses [5]. The latter behavior can have catastrophic consequences and it appears to depend on a variety of factors including composition [6], Poisson's ratio [6], temperature [7], and preparation [8,9]. Spatially, it corresponds to the emergence of a few-nanometers-thick shear band [10] in which most of the strain localizes while the material can remain cohesive. We seek to understand what aspects of the material ultimately control this discontinuous response and how shear bands nucleate.

At a microscopic level, plasticity takes place by discrete events, the so-called shear transformations, where a few particles rearrange locally [11–14]. The stress change it induces is anisotropic and long-range [14,15] and can in turn trigger new plastic events, generating anisotropic avalanches of plasticity [16,17]. It has been argued that amorphous solids are critical: Plasticity in the solid phase occurs via avalanches that can be system spanning [18–20]. Yet it is unclear if these avalanches of plasticity are precursors of discontinuous failure [21,22].

Recently, novel algorithms have been able to generate very stable glasses that show a discontinuous stress drop. This previously impossible feat was achieved by obtaining quench rates comparable to experiments [23,24] using swap algorithms [25,26] or by shearing the system back and forth many times [27]. These studies underline the critical role of system preparation in controlling a discontinuity in the stress response during loading. Theoretically, it was recently proposed that the yielding transition is a spinodal decomposition [28,29], which occurs, for example, in a magnet if a field is applied in the direction opposed to its magnetization. The magnetization can evolve smoothly or very suddenly (discontinuously), depending on the amount of disorder [30,31]. This analogy explains why increasing the initial stability of the glass can lead to a transition from a smooth to a discontinuous stress versus strain curve [23]. Yet, it does not incorporate the anisotropy of the interaction between shear transformations that causes shear bands nor the criticality of the solid phase. Other approaches based on shear transformation zones emphasize the role of system preparation in affecting yielding [32,33] but do not capture avalanches nor the possibility to have discontinuous stress versus strain curves. By contrast, a description based on plastic damage accumulation [34] can generate a macroscopic failure [35] but neglects the role of system preparation and anisotropic elastic interactions.

In this article, we first show that the transition between smooth and discontinuous stress versus strain curve is well captured by elastoplastic models [14] by increasing the stability of the initial configurations. We explain this observation in a mean-field approximation where the transition is found to be continuous, and failure can indeed be anticipated from the distribution of avalanches. However, these results break down for very stable glasses in finite dimensions due to rare locations in the sample where a shear band nucleates. To understand the physics of shear band nucleation, we then build an analogy with fracture mechanics. We predict that failure occurs if the spatial extension a of a weak region in the sample exceeds $a_c \sim (\Sigma - \Sigma_b)^{-2}$, where Σ is the stress and Σ_b is the stress that a shear band can carry. We confirm these results in an elastoplastic model, both by measuring the effect of inserting a defect in the material and by studying finite-size effects, which we argue are due to spontaneous occurrence of such defects. Overall, the framework we propose for how amorphous solids yield in quasistatic athermal conditions ties together the onset of sudden failure, avalanche statistics, and shear band nucleation in very stable materials.

*marko.popovic@epfl.ch
†matthieu.wyart@epfl.ch

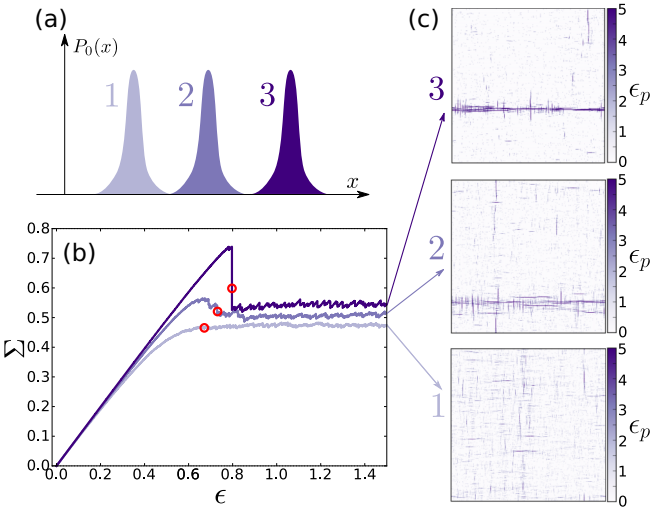

FIG. 1. An elastoplastic model can be continuous without (1) and with (2) a stress overshoot or be discontinuous (3), depending on the preparation. (a) Schematic of the initial distribution of stabilities, $P_0(x)$, representing the three system preparations. (b) Stress versus strain curves for these three different $P_0(x)$ together with snapshots of the spatial distribution of plastic strain ϵ_p. (c) Snapshots of the plastic strain taken at the positions indicated by red circles on the stress versus strain curves. (1) If the system preparation is not very stable, strain remains homogeneous and there is no stress overshoot. (2) As the stability of the preparation is increased a shear band is formed. (3) For a very stable preparation, a sharp shear band is formed during the macroscopic stress drop.

Discontinuous stress response in elastoplastic models. In elastoplastic models [14,36,37] the material is divided into N elements, each characterized by its shear stress σ_i and yield stress σ_i^Y. The overall stress of the system is simply $\Sigma = \sum_i \sigma_i/N$. When $|\sigma_i|$ reaches σ_i^Y, the element yields: After a time $\tau = 1$ its stress decreases by a value $\delta\sigma_i$, corresponding to a plastic deformation $\delta\epsilon_{p,i} = \delta\sigma_i/\mu_0$, where μ_0 is the shear modulus. New random variables σ_i and σ_i^Y are then taken from some distributions $P(\sigma)$ and $P_Y(\sigma^Y)$. Such a plastic event affects the stress everywhere in the material, according to a propagator $G(\vec{r})$ whose sign varies in space and which decays in magnitude as a dipole [14,37,38]. The specific parameters we use are described in the appendix. Such models have a finite macroscopic yield stress Σ_c, so that the material is solid for $|\Sigma| < \Sigma_c$ and liquid for $|\Sigma| > \Sigma_c$ [14]. In the solid case, these models predict how Σ depends on the accumulated plastic strain $\epsilon_p = \sum_i \epsilon_{p,i}/N$.

As the stress Σ is increased, most elements yield by reaching $\sigma_i = +\sigma_i^Y$. Therefore, it is useful to characterize elements by their stability $x_i = \sigma_i^Y - \sigma_i$. Depending on the initial distribution of stability $P_0(x)$, the stress was found to overshoot or not [18,39]. However, a discontinuous macroscopic stress drop has not been reported within these models.

We proceed by increasing the stability of the distribution $P_0(x)$ as illustrated in Fig. 1(a). For weakly stable initial states (case 1), the strain is homogeneous and the stress does not overshoot. When the initial stability is increased (case 2 in Fig. 1) the stress versus strain curve does display an overshoot. Although there is no macroscopic drop of stress, avalanches

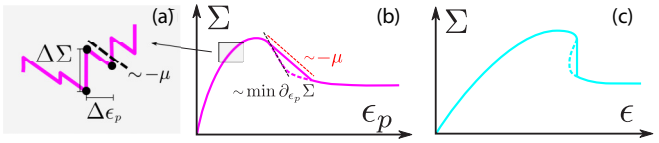

FIG. 2. (a) Stress versus plastic strain curve consists of alternating elastic stress increases $\Delta\Sigma$ and stress relaxations by an avalanche of plastic events $\Delta\Sigma_{\text{avalanche}} = -\mu\Delta\epsilon_p$. (b) When the slope of the macroscopic stress versus plastic strain curve reaches $-\mu$, an extensive avalanche occurs. (c) Stress versus strain curve corresponding to the stress versus plastic strain curve from panel (b) during a strain-controlled loading.

tend to localize along a rather thin shear band [40], as justified in Refs. [32,41].

A key observation is that for very stable systems, the scenario changes: The stress versus strain curve becomes discontinuous (case 3 in Fig. 1). A very narrow shear band appears in one single avalanche and relaxes the stress by some finite amount which persists in the thermodynamic limit; see below. This result supports that macroscopic failure can occur even in the absence of inertia and thermal feedback (in which strain increases temperature locally, which in turn localizes strain further), as these effects are absent in our model.

Avalanches and macroscopic failure. To explain this finding, we first consider the relationship between the avalanche size $S \equiv N\Delta\epsilon_p$, where $\Delta\epsilon_p$ is the total plastic strain accumulated during the avalanche, and the stress versus strain curve. When elements in the system begin to fail and the system deforms plastically, $P(x)$ develops a pseudogap $P(x) \sim x^\theta$ with $\theta > 0$ [42–44]. This result implies in turn that the minimal stability in the entire system [characterizing the size of the elastic ramps in Fig. 2(a)] follows $x_{\min} \sim N^{-1/(1+\theta)}$ [44], which was shown to constrain avalanche statistics for stress-controlled loading [18].

We generalise this result by noting that controlling stress is a special case of a more general loading protocol in which a spring of elasticity μ_S is placed between the system and a strain controlled loading apparatus. Stress controlled loading then corresponds to $\mu_S \to 0$ and strain controlled loading to $\mu_S \to \infty$. The overall shear elastic constant of this combined system is $\mu = \mu_0\mu_S/(\mu_0 + \mu_S)$, equivalent to a serial connection of two springs with elastic constants μ_0 and μ_S. In experiments μ_S has a finite value, which places them between these limit cases. Consider an increment of stress $\Delta\Sigma = x_{\min}$ followed by an avalanche where the stress drops by $\Delta\Sigma_{\text{avalanche}} = -\mu\Delta\epsilon_p$, which appears as a kink highlighted by the three black points in Fig. 2(a). Requiring that on average this kink has an overall slope $\partial\Sigma/\partial\epsilon_p \approx \langle\Delta\Sigma - \Delta\Sigma_{\text{avalanche}}\rangle/\langle\Delta\epsilon_p\rangle$, and using the definition of S as well as the scaling for $\langle x_{\min}\rangle$, it follows that

$$\langle S\rangle \sim \frac{N^{\frac{\theta}{\theta+1}}}{1 + \frac{1}{\mu}\frac{\partial\Sigma}{\partial\epsilon_p}}. \tag{1}$$

There are two key consequences that emerge from Eq. (1). (i) $\partial\Sigma/\partial\epsilon_p = -\mu$ is a sufficient condition for macroscopic failure (not always necessary, see below). Thus, if the spring μ_S is stiff, macroscopic failure is less likely: In particular,

if $\min_{\epsilon_p} \partial\Sigma/\partial\epsilon_p > -\mu$, we predict no macroscopic failure. (ii) The mean avalanche size generically diverges with N, signaling crackling noise and system-spanning avalanches even away from failure. This result is qualitatively different from disordered magnets [30], where the approach to failure is required for crackling to occur. However, the denominator in Eq. (1) diverges as the criterion $\partial\Sigma/\partial\epsilon_p \to -\mu$ is approached, suggesting that failure may be anticipated by monitoring avalanches.

Henceforth, we shall focus on the strain-controlled protocol, where Eq. (1) becomes

$$\langle S\rangle \sim N^{\frac{\theta}{\theta+1}}\left(1-\frac{1}{\mu}\frac{\partial\Sigma}{\partial\epsilon}\right), \tag{2}$$

where ϵ is the total strain $d\epsilon = d\epsilon_p + d\Sigma/\mu$. Then a sufficient condition for failure is that the stress versus strain curve develops an infinite slope, as illustrated in Fig. 2(c). Interestingly, it is still possible to probe this curve when it overhangs, if we allow the setup to have a negative stiffness $\mu_S < 0$, as is the case in the formalism we now develop.

Mean-field approximation. Following the previous paragraph, a discontinuous stress drop can be predicted by computing $\partial\Sigma/\partial\epsilon_p$. This is very hard in general because the mechanical noise generated by shear transformations is highly correlated in space. Mean-field approximations neglect these correlations [45]. In its simplest form, the mechanical noise is assumed to be white, corresponding to the Hebraud-Lequeux model [45]. In more realistic mean-field models, the noise is much broader, which leads to better values for the pseudogap exponent θ [43]. For our present purpose, however, we expect, and have checked numerically, that the two models lead to qualitatively similar behavior. We thus consider the simpler Hebraud-Lequeux model.

For simplicity, we assume yield stresses to be identical for all elements. We thus set $\sigma^Y = 1$. We further assume that locally the material is fully plastic, so that $\sigma_i \to 0$ and $x_i \to 1$ once element i yields. Thus $x_i = 0$ and $x_i = 2$ corresponds to the limit of stability of elements and elements that have yielded are reintroduced at $x_i = 1$. With this notation, the total stress is

$$\Sigma = 1 - \int_0^2 x\,P(x)dx. \tag{3}$$

The dynamical equation for the stability distribution $P(x)$ is a diffusion equation [45]

$$\partial_\gamma P(x,\gamma) = D\partial_x^2 P(x,\gamma) + v\partial_x P(x,\gamma) + \delta(x-1). \tag{4}$$

Here, $\gamma \equiv \epsilon_p\mu/\sigma^Y$ is number of plastic events per element, D characterizes the amplitude of the mechanical noise, and the source term describes the reinsertion of elements that have yielded. The drift v is a Lagrange multiplier that allows us to impose quasistatic loading. It is prescribed as follows: During quasistatic loading, no elements are unstable in the thermodynamic limit, implying the boundary conditions $P(0) = P(2) = 0$. This condition precludes failure, which will instead be signaled by an overhanging stress versus strain curve. By integrating Eq. (4), we find that $\partial_x P(2,\gamma) - \partial_x P(0,\gamma) = -1/D$. In practice, the first term becomes very small as soon as the stress rises [43] because almost no sites yield in the "wrong" direction at $x = 2$. Therefore, we can neglect the first term so that $\partial_x P(0,\gamma) = 1/D$. Taking the derivative of the stress, we now find

$$\partial_\gamma\Sigma = -1 + v = -1 - D^2\partial_x^2 P(0,\gamma), \tag{5}$$

where we evaluated Eq. (4) at $x = 0$ to find $v = -D\partial_x^2 P(0,\gamma)/\partial_x P(0,\gamma)$. Using Eqs. (4) and (5), $P(x)$ can be computed for any given $P_0(x)$, allowing us to compute $\Sigma(\gamma)$ from Eq. (5).

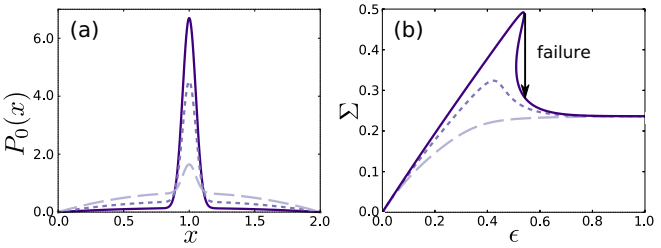

FIG. 3. (a) Initial stability distributions $P_0(x) \sim (1-\alpha)\exp[-(x-1)^2/(2s_P^2)] + \alpha x(2-x)$ with $s_P = 0.05$ we use to find (b) stress versus strain curves in the Hebraud-Lequeux model, showing the onset of macroscopic stress drop as the initial stability distribution $P_0(x)$ is narrowed.

We demonstrate the existence of a transition between smooth and discontinuous stress versus strain curves using as initial stability distribution $P_0(x) \sim (1-\alpha)\exp[-(x-1)^2/(2s_P^2)] + \alpha x(2-x)$, where $s_P = 0.05$ is kept constant and the distribution is normalized to 1 on the interval $x \in [0,2]$, as shown in Fig. 3(a). For $\alpha = 0.4$ the stress does not overshoot, while for $\alpha = 0.02$ the system shows a sudden drop in stress. At an intermediate value $\alpha = 0.08$, the system is still smooth but the stress overshoots, as shown in Fig. 3(b). Since $P_0(x)$ changes smoothly with α, there has to be an α_c at which the macroscopic stress drop occurs. This transition is continuous and of the usual saddle-node type, so that the magnitude of the stress jump scales as $\Delta\Sigma \sim (\alpha_c - \alpha)^{1/2}$. The same exponents are found in mean-field disordered magnets [23,31]. However, avalanches behave differently than in magnets: From Eq. (1) and the smoothness of the $\Sigma(\epsilon)$ curve, we get $\langle S\rangle \sim \sqrt{N}/\sqrt{\epsilon_c - \epsilon}$, where ϵ_c is the strain at which the stress drop occurs. Avalanche statistics can thus be used to forecast ϵ_c.

Our results have an interesting microscopic interpretation in terms of avalanches: From Eqs. (1) and (5), we obtain that $\langle S\rangle \sim -\sqrt{N}/\partial_x^2 P(0)$ for $\partial_x^2 P(0) < 0$ and it diverges otherwise. The avalanche size is thus controlled by the curvature of $P(x)$ at $x = 0$, whereby the failure occurs when this curvature vanishes. This result can be rationalized by a simple scaling argument following ideas from Ref. [46]. When an avalanche is initiated, the instantaneous number of unstable elements n_u evolves at each plastic event, and the avalanche ends when n_u returns to 0. If $P(x) = x/D$, during each plastic event one element is stabilized and on average one element becomes unstable. Therefore, n_u performs a simple random walk and there is no cutoff S_c in the avalanche size distribution. However, if the quadratic term is finite, $P(x) = x/D + \partial_x^2 P(0)x^2/2$ and a drift appears in the evolution of n_u. When $\partial_x^2 P(0) < 0$, on average less than one element becomes unstable per plastic event and the drift is negative. S_c corresponds to the avalanche size where the integrated

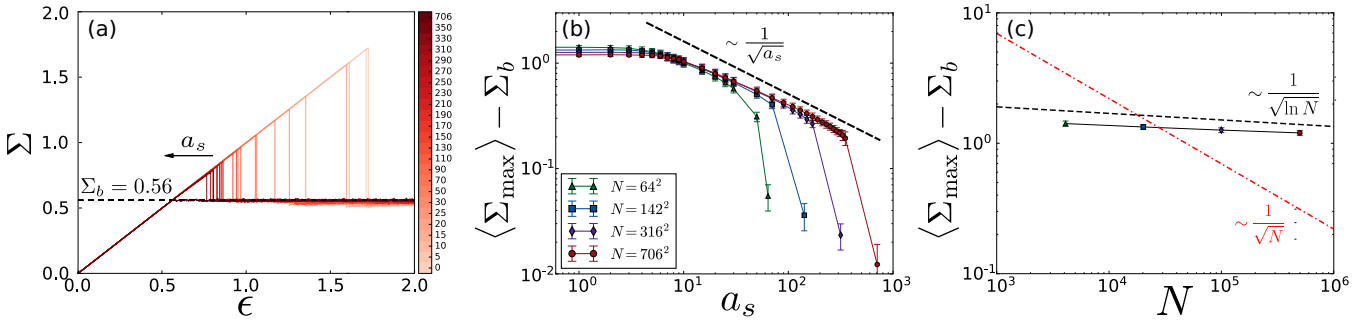

FIG. 4. (a) Stress versus strain curve in an elastoplastic model with $N = 706^2$ in which a defect of varying size a_s (as indicated in color) was inserted. (b) Maximal stress reached $\Sigma_{\max}$ as a function of the defect length a_s. (c) When no defects are inserted, $\Sigma_{\max}$ decreases very slowly with N, consistent with our prediction $\Sigma_{\max} - \Sigma_b \sim 1/\sqrt{\ln N}$.

drift $-N \int_0^{x_c} \partial_x^2 P(0) x^2 dx$ is of the order of fluctuations $S_c^{1/2}$. Here, $x_c \sim \sqrt{2DS_c/N}$ is the characteristic value of the initial stability of elements that became unstable in the avalanche. We thus obtain $S_c \sim -N^{1/2}/\partial_x^2 P(0)$: The negative curvature of $P(x)$ at $x = 0$ determines the avalanche size by depleting the pool of elements that can become unstable.

Nucleation of shear band. We now argue that for initially very stable systems at least, macroscopic failure can occur without the apparent divergence of avalanche size described by Eq. (1) and thus cannot be easily anticipated by a growing crackling noise. Instead, a shear band can nucleate in a region which, by chance, is weaker than the rest of the material. Consider a region of dimension $d-1$, where d is the spatial dimension, and of linear extension a that has already yielded and thus has smaller yield stresses than the rest of the material. We denote by Σ_b the shear stress such a narrow shear band can sustain in the limit of large a (Σ_b can in general depend on system preparation). If $\Sigma > \Sigma_b$, the stress will be distorted by this weak region. This is a classical calculation of fracture mechanics [47], leading to a stress at a distance r to the tip of the shear band of order

$$\Sigma(r) \sim \frac{(\Sigma - \Sigma_b)\sqrt{a}}{\sqrt{r}} \equiv \frac{\mathcal{K}}{\sqrt{r}}, \tag{6}$$

where $\mathcal{K}$ is known as the stress intensity factor. In analogy with fracture mechanics, we expect the shear band to propagate if $\mathcal{K}$ is larger than some critical value $\mathcal{K}_c$, leading to a critical nucleus size a_c triggering failure:

$$a_c \sim \frac{1}{(\Sigma - \Sigma_b)^2}. \tag{7}$$

Equation (7) is easily tested in the elastoplastic model by inserting a defect, i.e., a region with unusually small yield stresses of extension a_s. This procedure is analogous to the introduction of a void in a material, as is often used to measure its fracture toughness [47]. From Eq. (7), we expect a discontinuous stress drop to occur for some $\Sigma_{\max}$ satisfying $\Sigma_{\max} - \Sigma_b \sim 1/\sqrt{a_s}$. This prediction is confirmed in Figs. 4(a) and 4(b).

In a large, homogeneously prepared system, spontaneous shear bands will occur. The probability to find a weak region of spatial extension a follows $p(a) \sim N \exp(-a^{d-1})$, the largest weak region formed by chance follows $a \sim (\ln N)^{1/(d-1)}$. Together with Eq. (7), this leads to $\Sigma_{\max} - \Sigma_b \sim 1/(\ln N)^{1/(2(d-1))}$. This decay is so weak that even for N of the order of the Avogadro number, we expect the overshoot to be significant. It is hard to test this asymptotic result numerically. However we find that for the elastoplastic model, the dependence of $\Sigma_{\max}$ with N is consistent with the slow decay predicted, as shown in Fig. 4(c). The data exclude the more rapid decay $1/\sqrt{N}$ expected from a naive central limit theorem argument.

Conclusion. The response of a material to loading is one of its most practically important properties. We have shown that elastoplastic models can reproduce a transition between a smooth and discontinuous stress response in amorphous solids as their initial stability is increased, in agreement with experimental and recent numerical observations. We have explained this result in a mean-field approximation, in which macroscopic failure can always be predicted by a growing crackling noise. We have argued, however, that for very stable materials, failure is induced by rare events in which a shear band nucleates, which cannot be forecasted, and we have provided a theoretical description of this nucleation.

Our work suggests interesting venues for further theoretical and experimental studies. As illustrated in Fig. 1(c)(2), shear bands formed during the continuous overshoot of stress are broader than the ones formed during the discontinuous stress change. It is unclear if their formation can be described in terms of fracture mechanics or if it is instead associated with crackling noise as in mean field. This point could be investigated systematically in terms of relevant parameters, including system preparation, loading apparatus, as well as strain rate and temperature.

Acknowledgments. We thank L. Berthier, G. Biroli, M. Ozawa, G. Tarjus, and A. Rosso for sharing unpublished results and discussions and the Simons collaboration for discussions. M.W. thanks the Swiss National Science Foundation for support under Grant No. 200021-165509 and the Simons Foundation Grant No. 454953. T.G. was partly financially supported by The Netherlands Organisation for Scientific Research (NWO) by NWO Rubicon Grant No. 680-50-1520. We acknowledge open-source software: the SciPy ecosystem [48] and GNU parallel [49].

APPENDIX: IMPLEMENTATION OF THE ELASTOPLASTIC MODEL

We implement a two-dimensional elastoplastic model on a periodic lattice of sizes $L = 64, 142, 316, 706$. The propaga-

tor $G(r,\phi)$ is a periodic version of an infinite system propagator $G_0(r,\phi) \sim \cos 4\phi/r^2$ and it is normalized so that $G(\vec{r}=0)=-1$. This propagator preserves the sum of stresses along each row and column of elements.

To keep the sum of stresses in all rows and columns the same during the initialization of the stress distribution $P(\sigma)$, we proceed as follows. We start with 0 stress in each element. Then, for each element i, we draw a random stress $\delta\sigma$ from a normal distribution $\mathcal{N}(0, s_0^2)$ and we draw two random integer numbers δx and δy between 1 and the system's length L. Then we add the stress $\delta\sigma$ to element i and the element at coordinates $(x_i-\delta x, y_i-\delta y)$ and we subtract $\delta\sigma$ from the stresses of elements at positions $(x_i-\delta x, y_i)$ and $(x_i, y_i-\delta y)$. Periodicity is imposed when needed. Finally, since on average each element has received a stress update four times by a random number drawn from a normal distribution of variance s_0^2, we divide the stress of all elements by 2 to keep the variance of the initial stress distribution equal to s_0^2. We use $s_0=0.45$ in Fig. 1 and $s_0=0.3$ in Fig. 4.

The initial distribution of yield stresses $P(\sigma^Y)$ is a normal distribution $\mathcal{N}(m, 0.01)$. In cases 1, 2 and 3 in Fig. 1 we use $m=1.3, 1.5, 1.8$. In Fig. 4, $m=3.0$ except in defect, where $m=1.0$.

After a plastic failure, the yield stress of the element is updated with a random number from a normal distribution $\mathcal{N}(1, 0.01)$, and the stress of the element is set to a random value drawn from a normal distribution $\mathcal{N}(0, 0.01)$.

Timescale τ represents a mean time it takes for an unstable element to yield and the probability density to yield is uniform in time. Note that an unstable element can be stabilized if its stress becomes $|\sigma_i| < \sigma^Y$ before it yields.

[1] P. Johnson and X. Jia, Nature (London) **437**, 871 (2005).
[2] J. Schroers and W. L. Johnson, Phys. Rev. Lett. **93**, 255506 (2004).
[3] D. Bonn, M. Denn, L. Berthier, T. Divoux, and S. Manneville, Rev. Mod. Phys. **89**, 035005 (2017).
[4] B. Andreotti, Y. Forterre, and O. Pouliquen, *Granular Media: Between Fluid and Solid* (Cambridge University Press, Cambridge, UK, 2013).
[5] J. Antonaglia, X. Xie, G. Schwarz, M. Wraith, J. Qiao, Y. Zhang, P. Liaw, J. Uhl, and K. Dahmen, Sci. Rep. **4**, 4382 (2015).
[6] J. Lewandowski, W. Wang, and A. Greer, Philos. Mag. Lett. **85**, 77 (2005).
[7] J. Lu, G. Ravichandran, and W. L. Johnson, Acta Mater. **51**, 3429 (2003).
[8] Y. Shi and M. L. Falk, Phys. Rev. Lett. **95**, 095502 (2005).
[9] X. Gu, S. Poon, G. Shiflet, and J. Lewandowski, Scr. Mater. **60**, 1027 (2009).
[10] Y. Zhang and A. Greer, Appl. Phys. Lett. **89**, 071907 (2006).
[11] A. Argon, Acta Metall. **27**, 47 (1979).
[12] M. L. Falk and J. S. Langer, Phys. Rev. E **57**, 7192 (1998).
[13] P. Schall, D. Weitz, and F. Spaepen, Science **318**, 1895 (2007).
[14] A. Nicolas, E. Ferrero, K. Martens, and J.-L. Barrat, arXiv:1708.09194.
[15] G. Picard, A. Ajdari, F. Lequeux, and L. Bocquet, Eur. Phys. J. E **15**, 371 (2004).
[16] A. Lemaître and C. Caroli, Phys. Rev. Lett. **103**, 065501 (2009).
[17] C. E. Maloney and M. O. Robbins, Phys. Rev. Lett. **102**, 225502 (2009).
[18] J. Lin, T. Gueudré, A. Rosso, and M. Wyart, Phys. Rev. Lett. **115**, 168001 (2015).
[19] M. Müller and M. Wyart, Annu. Rev. Condens. Matter Phys. **6**, 177 (2015).
[20] Z. Budrikis, D. Castellanos, S. Sandfeld, M. Zaiser, and S. Zapperi, Nat. Commun. **8**, 15928 (2017).
[21] F. Gimbert, D. Amitrano, and J. Weiss, EPL **104**, 46001 (2013).
[22] A. Le Bouil, A. Amon, S. McNamara, and J. Crassous, Phys. Rev. Lett. **112**, 246001 (2014).
[23] M. Ozawa, L. Berthier, G. Biroli, A. Rosso, and G. Tarjus, Proc. Natl. Acad. Sci. U.S.A. **115**, 6656 (2018).
[24] Y. Jin, P. Urbani, F. Zamponi, and H. Yoshino, arXiv:1803.04597.
[25] A. Ninarello, L. Berthier, and D. Coslovich, Phys. Rev. X **7**, 021039 (2017).
[26] C. Brito, E. Lerner, and M. Wyart, Phys. Rev. X **8**, 031050 (2018).
[27] P. Leishangthem, A. Parmar, and S. Sastry, Nat. Commun. **8**, 14653 (2017).
[28] C. Rainone, P. Urbani, H. Yoshino, and F. Zamponi, Phys. Rev. Lett. **114**, 015701 (2015).
[29] G. Parisi, I. Procaccia, C. Rainone, and M. Singh, Proc. Natl. Acad. Sci. U.S.A. **114**, 5577 (2017).
[30] J. P. Sethna, K. Dahmen, S. Kartha, J. A. Krumhansl, B. W. Roberts, and J. D. Shore, Phys. Rev. Lett. **70**, 3347 (1993).
[31] S. K. Nandi, G. Biroli, and G. Tarjus, Phys. Rev. Lett. **116**, 145701 (2016).
[32] M. L. Manning, J. S. Langer, and J. M. Carlson, Phys. Rev. E **76**, 056106 (2007).
[33] M. Vasoya, C. H. Rycroft, and E. Bouchbinder, Phys. Rev. Appl. **6**, 024008 (2016).
[34] C. B. Picallo, J. M. López, S. Zapperi, and M. J. Alava, Phys. Rev. Lett. **103**, 225502 (2009).
[35] C. B. Picallo, J. M. López, S. Zapperi, and M. J. Alava, Phys. Rev. Lett. **105**, 155502 (2010).
[36] J.-C. Baret, D. Vandembroucq, and S. Roux, Phys. Rev. Lett. **89**, 195506 (2002).
[37] G. Picard, A. Ajdari, F. Lequeux, and L. Bocquet, Phys. Rev. E **71**, 010501 (2005).
[38] V. Démery, V. Dansereau, E. Berthier, L. Ponson, and J. Weiss, arXiv:1712.08537.
[39] E. Jagla, Phys. Rev. E **76**, 046119 (2007).
[40] D. Vandembroucq and S. Roux, Phys. Rev. B **84**, 134210 (2011).

[41] R. L. Moorcroft and S. M. Fielding, Phys. Rev. Lett. **110**, 086001 (2013).
[42] J. Lin, A. Saade, E. Lerner, A. Rosso, and M. Wyart, EPL **105**, 26003 (2014).
[43] J. Lin and M. Wyart, Phys. Rev. X **6**, 011005 (2016).
[44] S. Karmakar, E. Lerner, and I. Procaccia, Phys. Rev. E **82**, 055103 (2010).
[45] P. Hébraud and F. Lequeux, Phys. Rev. Lett. **81**, 2934 (1998).
[46] E. Jagla, Phys. Rev. E **92**, 042135 (2015).
[47] T. Anderson, *Fracture Mechanics, Fundamentals and Applications*, 3rd ed. (CRC Press, Boca Raton, FL, 2005).
[48] E. Jones, T. Oliphant, P. Peterson, and Others, SciPy: Open source scientific tools for PYTHON, http://www.scipy.org/.
[49] O. Tange, login: The USENIX Magazine **36**, 42 (2011).